

Daylight Vision Repair by Cell Transplantation

TIAGO SANTOS-FERREIRA,^a KAI POSTEL,^a HENRIKE STUTZKI,^{b,c} THOMAS KURTH,^a GÜNTHER ZECK,^b MARIUS ADER^a

Key Words. Retinal degeneration • Transplantation • Cone-like photoreceptor • Nrl-deficient mouse • Microelectrode array

ABSTRACT

Human daylight vision depends on cone photoreceptors and their degeneration results in visual impairment and blindness as observed in several eye diseases including age-related macular degeneration, cone-rod dystrophies, or late stage retinitis pigmentosa, with no cure available. Preclinical cell replacement approaches in mouse retina have been focusing on rod dystrophies, due to the availability of sufficient donor material from the rod-dominated mouse retina, leaving the development of treatment options for cone degenerations not well studied. Thus, an abundant and traceable source for donor cone-like photoreceptors was generated by crossing neural retina leucine zipper-deficient ($Nrl^{-/-}$) mice with an ubiquitous green fluorescent protein (GFP) reporter line resulting in double transgenic $tg(Nrl^{-/-}; aGFP)$ mice. In $Nrl^{-/-}$ retinas, all rods are converted into cone-like photoreceptors that express CD73 allowing their enrichment by CD73-based magnetic activated cell sorting prior transplantation into the subretinal space of adult wild-type, cone-only ($Nrl^{-/-}$), or cone photoreceptor function loss 1 ($Cpf1$) mice. Donor cells correctly integrated into host retinas, acquired mature photoreceptor morphology, expressed cone-specific markers, and survived for up to 6 months, with significantly increased integration rates in the cone-only $Nrl^{-/-}$ retina. Individual retinal ganglion cell recordings demonstrated the restoration of photopic responses in cone degeneration mice following transplantation suggesting, for the first time, the feasibility of daylight vision repair by cell replacement in the adult mammalian retina. *STEM CELLS* 2015;33:79–90

INTRODUCTION

Human vision depends mainly on daylight vision and degeneration of the responsible cells, cone photoreceptors, leads to severe visual impairment. Several retinal diseases affecting cones such as age-related macular degeneration (AMD), cone-rod dystrophies, or late-stage retinitis pigmentosa (RP) result in clinical pathophysiology characterized by progressive loss of cone photoreceptors. Cone photoreceptors mediate daylight and color vision, visual acuity, and their degeneration ultimately leads to blindness with no treatments established [1, 2]. The adult mammalian retina, including humans, does not intrinsically regenerate and thus dying photoreceptors result in permanent vision loss. Several therapeutic approaches are currently being developed to treat retinal degenerative diseases [3, 4]. However, most require the existence of target cells and despite indications for visual improvements a continuous degeneration of photoreceptors was observed [5].

Cell-based therapies aiming to replace lost photoreceptors represent a promising alternative and potentially general treatment strategy.

Proof-of-concept studies demonstrated the feasibility of rod photoreceptor transplantation into the adult mouse retina leading to correct integration of donor photoreceptors and restoration of visual function in RP mouse models [6–8]. However, these preclinical studies are mainly focused on rod photoreceptor degenerations [9–18] due to the availability of sufficient donor material from the rod-dominated mouse retina.

Therefore, very little is known about cone photoreceptor transplantation [19] and its potential for functional rescue. In the mouse retina only ~3% of all photoreceptors are cones [20], representing a limited source of donor cells for transplantation. Interestingly, deficiency in the transcription factor neural retina leucine zipper ($Nrl^{-/-}$) in mice results in the generation of rod-depleted retinas containing solely cone and cone-like photoreceptors [21]. The $Nrl^{-/-}$ mouse was characterized in detail showing that cone-like cells resemble blue (s-) cones at the morphological and functional level [21, 22].

Here, using $Nrl^{-/-}$ mice as an abundant source of donor cells, we demonstrated the feasibility of cone-like photoreceptor enrichment

^aCRTD/DFG-Center for Regenerative Therapies Dresden, Technische Universität Dresden, Dresden, Germany; ^bNatural and Medical Sciences Institute at the University of Tübingen, Reutlingen, Germany; ^cGraduate Training Centre of Neuroscience, Tübingen, Germany.

Correspondence: Marius Ader, PhD, CRTD/DFG-Center for Regenerative Therapies Dresden, Technische Universität Dresden, Fetscherstraße 105, 01307 Dresden, Germany. Telephone: 49-351-458-82203; Fax: 49-351-458-82219; e-mail: marius.ader@crt-dresden.de

Received March 14, 2014; accepted for publication August 6, 2014; first published online in *STEM CELLS EXPRESS* September 2, 2014.

© AlphaMed Press
1066-5099/2014/\$30.00/0

<http://dx.doi.org/10.1002/stem.1824>

and transplantation into the adult mouse retina. Transplanted cone-like photoreceptors showed correct integration and maturation within the host tissue, expression of cone-specific markers, and survival for up to 6 months. Importantly, integrated donor cells restored daylight responses after transplantation into a mouse model of cone degeneration. These results emphasize the feasibility of cell replacement strategies for retinal degenerations affecting cone photoreceptors.

MATERIALS AND METHODS

Animal Experimentation

Adult age-matched (6–9 weeks) wild-type (C57BL/6J), $Nrl^{-/-}$ [21], and cone photoreceptor function loss 1 (Cpfl1) [23] mutant mice were used as recipients for cell transplantation. A donor cell source was generated by crossing Nrl -deficient ($Nrl^{-/-}$) mice with an actin-green fluorescent protein (GFP) mouse line [24]. The resulting mouse line, $tg(Nrl^{-/-}; aGFP)$, was used as a donor cell source after detailed characterization. Donor cells were obtained from P1 to P8 $tg(Nrl^{-/-}; aGFP)$ mice. All animal experiments were approved by the ethics committee of the TU Dresden and the Landesdirektion Dresden (approval number: 24D-9168.11-1/2008-33). All regulations from European Union, German laws (Tierschutzgesetz), the ARVO statement for the Use of Animals in Ophthalmic and Vision Research and the NIH Guide for the care and use of laboratory work were strictly followed for all animal work. Experimental animals were housed in the animal facility at the Medical Theoretical Center of the Technische Universität Dresden.

Semiquantitative RT-PCR

RNA from $tg(Nrl^{-/-}; aGFP)$ and C57BL/6J retinas was isolated using RNeasy Minikit (Qiagen, Hilden, Germany, www.qiagen.com/) according to the manufacture instructions. cDNA was generated using reverse transcriptase Superscript II RT kit (Qiagen) according to the manufactures instructions. Primers and respective annealing temperatures used are described in Supporting Information Table S1.

Electroretinogram

Electroretinogram (ERG) recordings were performed in 9-week-old C57BL/6J, Cpfl1 mutant, and $Nrl^{-/-}$ mice using a SuperColor Ganzfeld Q450SC (Roland Consult, Brandenburg an der Havel, Germany, www.roland-consult.de) and all mouse handling was performed in a dark room under dim red light. Experimental animals were dark-adapted (>12 hours), anesthetized with an intraperitoneal injection of medetomidine hydrochloride (0.01 mg/10 g b.wt., Dormitor, Pfizer, Berlin, Germany, www.pfizer.de) and ketamine (0.75 mg/10 g b.wt.; Ratiopharm, Ulm, Germany, www.ratiopharm.de), pupils dilated with 2.5% phenylephrine/0.5% tropicamide solution (TU Dresden Pharmacy, Dresden, Germany), and placed in the recording stage. A reference electrode was introduced under the skin and a ground electrode in the mouse's mouth, followed by gold-ring electrodes (Roland Consult) in close contact to the cornea. Visidic (Dr. Mann Pharma/Andrae-Noris Zahn AG, Berlin, Germany, www.bausch-lomb.de) was applied to the eye to ensure good electrical transmission and to keep the eye hydrated. Single-flash responses were recorded under

dark-adapted (scotopic) and light-adapted conditions (photopic). Single flash ERG was performed as follows: five single-flash stimuli with increasing intensities were presented to the experimental animal with 5 seconds (0.0003, 0.001, 0.003, 0.01, 0.03, 0.1 cd/m^2), 10 seconds (0.3 cd/m^2), or 17 seconds (1.0, 3.0, and 10.0 cd/m^2) interval between light-flash intensities. Light adaptation was performed using background illumination of 25 cd/m^2 for 10 minutes. The averaged recordings for each light stimulus were processed offline using a 50 Hz filter.

Magnetic-Activated Cell Sorting and Subretinal Transplantation into Mice

$tg(Nrl^{-/-}; aGFP)$ retinas were isolated at different developmental stages (P1, 4, 6, and 8), magnetic-activated cell (MAC)-sorted using CD73 antibody (BD Pharmingen, Heidelberg, Germany), and 1 μ l of MACS buffer containing 200,000 cells was injected into the subretinal space of host retinas as previously described in detail [25]. Briefly, mice were anesthetized with an intraperitoneal injection of medetomidine hydrochloride (0.01 mg/10 g b.wt., Dormitor, Pfizer) and ketamine (0.75mg/10g body weight; Ratiopharm) and pupils were dilated with 2.5% phenylephrine/0.5% tropicamide (TU Dresden Pharmacy). Following fixation in a head holder (Leica, Wetzlar, Germany, www.leica-microsystems.com/), a hole was made in the ora serrata with a sharp 30-gauge needle (VWR, Dresden, Germany, www.vwr.com). A blunt 34-Gauge needle connected to a 5 μ l Hamilton syringe was then transvitreally inserted into the eye under visual control, placed nasally in the subretinal space, and the cell suspension was slowly injected. Experimental eyes showing obvious damage of the retina and/or bleeding were discarded from further analysis. Control rod photoreceptor transplantation into Cpfl1 recipients was performed as described above but with donor cells isolated from Nrl -GFP mice [26]. For flow cytometry analyses, 300,000 cells from unsorted, CD73-positive and CD73-negative fractions were incubated with donkey anti-rat antibodies conjugated with APC Fluorophore (BD Biosciences, Heidelberg, Germany, www.bdbiosciences.com), washed in MACS buffer, spun down, resuspended in fluorescence-activated cell sorting buffer, and analyzed by LSR flow cytometer (BD Biosciences).

Tissue Processing and Immunohistochemistry

Experimental animals were sacrificed by cervical dislocation. Eucleated eyes were immediately washed in 70% ethanol solution and transferred to a Petri dish containing sterile Hank's Balanced Salt Solution (Life Technologies, Darmstadt, Germany, www.lifetechnologies.com). Using a sharp 30-Gauge 1/2" needle (BD Microlance 3, VWR), a hole was made in the ora serrata in the temporal region of the eye. Eyes were immediately transferred to a 4% paraformaldehyde (PFA) solution (Sigma-Aldrich, Munich, Germany, www.sigmaaldrich.com) for 1 hour at 4°C. The anterior region of the eye was then removed and the posterior part cryopreserved in a 30% (wt/vol) sucrose solution overnight at 4°C. Eyes were cut in two halves, embedded in NEG50 (Thermo Scientific, Schwerte, Germany, www.thermoscientific.com), and cryo-sectioned with 20 μ m thickness using a microtome (Micron HM560, Thermo Scientific). Frozen retinal sections were air-dried for 1 hour at room temperature (RT) and hydrated for 30 minutes in phosphate buffered saline (PBS) followed by blocking using 0.3%

Triton X-100 solution with 1% bovine serum albumin (BSA) and 5% donkey serum for 1 hour at RT. Specimen were incubated overnight at 4°C with the following primary antibodies: blue-opsin (1:200, SantaCruz, Heidelberg, Germany, www.scbt.com), cone arrestin (1:500, kindly provided by Wolfgang Baehr), peanut agglutinin (PNA) (1:500, Vector Laboratories, Peterborough, UK, www.vectorlabs.com), recoverin (1:5,000, Millipore, Schwalbach, Germany, www.merckmillipore.com), synaptophysin (1:1,000, Sigma-Aldrich), bassoon (1:1,000, Stressgen, San Diego, CA, www.stressgen.com), CD68 (1:500, Abcam, Cambridge, UK, www.abcam.com), secretagoin (1:2,000, Biovendor, Heidelberg, Germany, www.biovendor.com), calbindin (1:1,000, Abcam), and GFP (1:800, Abcam). Excess of primary antibody was removed by washing three times for 10 minutes in PBS. Corresponding secondary antibodies coupled to the fluorescent dyes Alexafluor 488, Alexafluor 546, Cy2, Cy3, or Cy5, at a dilution of 1:1,000, were incubated for 1 hour 30 minutes at RT together with 4',6-diamidino-2-phenylindole (DAPI; 1:20,000; Sigma). Immunocytochemistry for CD73 was performed on unfixed dissociated retinal cells plated on laminin-coated coverslips as previously described [13]. Retinal sections and plated cells on coverslips were preserved following immunocytochemistry using AquaPolymount (Polysciences, Heidelberg, Germany, www.polysciences.com) and further imaged using a Zeiss Apotome ImagerZ1 (Zeiss, Heidelberg, Germany, www.zeiss.de).

Quantification of Integrated Cone-Like Photoreceptors

Transplanted animals, in which there was less than 25% reflux after transplantation, were selected for further analysis and quantification. Host eyes were processed and stained for GFP and photoreceptor-specific markers. Every fourth serial section from whole experimental retinas was used to quantify the total amount of integrated photoreceptors. A transplanted cell was considered an integrated photoreceptor if it displayed one of the following morphological features: (a) cell body properly located in the outer nuclear layer (ONL) with projections ending in an inner segment (IS) and synaptic terminal; (b) cell body properly located in the ONL with IS or synaptic terminal; (c) cell body with one process toward the outer limiting membrane and one process toward the outer plexiform layer (OPL). Following the quantification of the integrated photoreceptors, the resulting value was multiplied by four to estimate the total amount of integrated donor cells per retina.

Correlative Light and Electron Microscopy

Transplanted Cpf1 retinas were fixed with 4% PFA in 0.1 M phosphate buffer (PB, pH 7.4), cut into small pieces under a fluorescence dissection microscope (Leica MZ10F), and processed for Tokuyasu cryo-sectioning as described [27, 28]. Briefly, the tissue pieces were washed several times in PB, infiltrated stepwise into 10% gelatin, and cooled down on ice. The blocks were incubated in 2.3 M sucrose/water for 24 hours at 4°C, mounted on Pins (Leica), and plunge frozen in liquid nitrogen. Sections (70 nm) were cut on a Leica UC6+FC6 cryo-ultramicrotome and picked up in methyl cellulose/sucrose (1 part 2% methyl cellulose [MC], Sigma-Aldrich, 25 cP + 1 part 2.3 M sucrose). To facilitate the identification of GFP-labeled cells, sections were stained for correlative light electron microscopy [29, 30]. Grids with sections were placed

upside down on drops of PBS in a 37°C-incubator for 20 minutes, washed with 0.1% glycyl/PBS (5 × 1 minute), blocked with 1% BSA/PBS (2 × 5 minutes), and incubated with primary antibodies for 1 hour (anti-GFP: TP 401, Torrey Pines, Secaucus, New Jersey, www.chemokine.com/ 1:100). After washes in PBS (4 × 2 minutes), the sections were incubated with Protein A conjugated to 10 nm gold for 1 hour, washed in PBS (3 × 5 seconds, 4 × 2 minutes), and postfixed in 1% glutaraldehyde (5 minutes). Subsequently, the sections were incubated with goat-anti-rabbit Alexa 488 for the identification of cone-like cells in the fluorescence microscope. After staining, sections were washed in PBS (4 × 2 minutes), stained with 1 µg/ml DAPI for 10 minutes, washed in water (10 × 1 minute), mounted in 50% glycerin/water between two coverslips, and imaged with a Keyence BZ8000 fluorescence microscope (Keyence, Neu-lsenburg, Germany, www.keyence.de). Then, sections were demounted, washed several times in water, and stained with neutral uranyl oxalate (2% uranyl acetate [UA] in 0.15 M oxalic acid, pH 7.0) for 5 minutes, washed shortly in water, and incubated in MC containing 0.4% UA for 5 minutes. Grids were looped out, the MC/UA film was reduced to an even thin film, and air dried. Finally, the sections were analyzed on a Philips Morgagni 268 (FEI, Eindhoven, The Netherlands, www.fei.com) at 80 kV and images were taken with the MegaView III digital camera (Olympus, Soft-Imaging Solutions, Münster, Germany, www.olympus-sis.com/).

Statistical Analyses and Image Processing

The resulting data were presented with mean ± SEM for at least three independent biological replicates. Statistical significance was calculated using a paired, two-tailed Student's *t* test or one-way ANOVA. Statistical significance was represented in the figures as follows: *, *p* < .05; **, *p* < .01; ***, *p* < .001; ****, *p* < .0005, n.s.: not-statistical significant. Images and graphs were processed and generated using Image J (National Institutes of Health), FlowJo, Axiovision Software (Zeiss), Adobe Photoshop CS5 (Adobe Systems Incorporated), and Microsoft Office 2011 (Microsoft Corporation).

Recording of Retinal Ganglion Cells

Extracellular recordings of retinal ganglion cells (RGCs) spiking activity were performed using planar and transparent microelectrode arrays (MEA; Multi Channel Systems, Reutlingen, Germany, www.multichannelsystems.com/) as recently reported [31]. Briefly, retinas of dark-adapted mice were isolated from the eye cup under dim red light illumination, cut in half, and placed ganglion cell side down on an electrode array comprising 252 electrodes (electrode diameter: 10 µm, electrode spacing: 60 µm). During recordings, the retina was continuously perfused with carbogenated Ames' medium (Sigma-Aldrich) and maintained at 35°C. Extracellular voltage traces were recorded using the filter settings of 0.3–3 kHz. The offline analysis of the high-pass filtered voltage traces comprised as a first step detection of threshold crossings (5 × electrode rms) and subsequent assignment of the extracellular waveforms to ganglion cells using Klustakwik [32]. The retina was stimulated using a LED (Luxeon, 505 nm) focused through the transparent MEA onto the photoreceptor layer. Periodic flashes were produced by switching the LED every 500 milliseconds between two light levels. For all stimulus protocols, the contrast was 0.97. Contrast was calculated

as $(I_{\text{on}} - I_{\text{off}})/(I_{\text{on}} + I_{\text{off}})$. The overall light level was set by a customized circuit driven by a stimulus generator (Multi Channel Systems). Recordings at three different light levels (10, 66, and 280 mW/m²) were performed in the order of increasing intensities. For technical reasons, the lowest light intensity was 10 mW/m². For each light level, a 10–15-minute adaptation period at constant illumination preceded the recordings.

RESULTS

Generation and Characterization of Cone-Like Photoreceptor Reporter Mice

By crossing *Nrl*^{-/-} mice with the ubiquitous reporter line actin-GFP (aGFP) [24], a double transgenic mouse line *tg(Nrl*^{-/-}; aGFP) was generated as a source of labeled cone-like photoreceptors for transplantation studies. Adult *tg(Nrl*^{-/-}; aGFP) mice displayed all hallmarks of the *Nrl*^{-/-} phenotype with rosettes located in the ONL, expression of cone-specific genes (PNA, s-opsin, and cone arrestin) in virtually all photoreceptors, and no expression of rod-specific genes like *Nrl* or rhodopsin (Supporting Information Fig. S1). ERG measurements revealed the lack of rod-mediated responses under low light (scotopic) conditions and similar b-wave amplitudes under cone-mediated bright light (photopic) conditions, however, with significantly increased latencies under mesopic and photopic conditions in *tg(Nrl*^{-/-}; aGFP) when compared with *Nrl*^{-/-} mice (Supporting Information Fig. S2).

Enrichment of Cone-Like Photoreceptors by CD73-Based MACS

Ecto-5'-nucleotidase (Nt5e or CD73) was identified as a marker of photoreceptors including rod and cone precursors beside mature rods and is transcriptionally located downstream of the cone-rod homeobox gene (*Crx*) [33]. Its usefulness as a cell surface antigen to enrich rod photoreceptors for transplantation studies was recently demonstrated [13, 17]. Published microarray data predicted the expression of CD73 also in cone-like photoreceptors of *Nrl*^{-/-} mice [26]. Thus, the expression of CD73 in retinas of the newly generated *tg(Nrl*^{-/-}; aGFP) mice was evaluated for subsequent enrichment of photoreceptors via MACS. Immunostaining of dissociated and plated postnatal day 4 (P4) *tg(Nrl*^{-/-}; aGFP) retinas revealed that 31.21% ± 1.85% (*n* = 3; mean ± SEM) of cells expressed CD73, displaying a membrane-like pattern (Supporting Information Fig. S3A, S3B). Next, using CD73-based MACS, P4 *tg(Nrl*^{-/-}; aGFP) retinal cells were sorted and the resulting fractions, that is, CD73-positive (CD73⁺) and CD73-negative (CD73⁻) fractions, were analyzed by flow cytometry and RT-PCR. A significant enrichment of cone-like photoreceptors in the CD73⁺ fraction (78.8% ± 1.3% [*n* = 3] [mean ± SEM]) was observed when compared with the input fraction (60.4% ± 0.5% [*n* = 3] [mean ± SEM]). In the CD73⁻ sorted fraction only 3.9% ± 0.8% (*n* = 3) (mean ± SEM) CD73⁺ cells were detected (Supporting Information Fig. S3C, S3D). Additionally, increased expression of photoreceptor-specific genes including *Crx* and s-opsin was observed in CD73⁺ fractions in comparison to CD73⁻ or unsorted fractions (Supporting Information Fig. S3E), confirming the feasibility of cone-like photoreceptor enrichment by CD73-based MACS. All subsequent transplantations were further performed using CD73⁺ cell fractions.

Cone-Like Photoreceptors Integrate in an Age-Dependent Fashion and Express Cone-Specific Markers

Nrl-deficiency leads to conversion of rods toward cone-like photoreceptors without disruption of overall retinal development. Thus, the peak of cone-like photoreceptor generation is not shifted toward embryonic stages, when cones are normally born, but remain at similar stages as for rods, that are mainly developing postnatally. Therefore, cone-like photoreceptors were isolated at different postnatal developmental stages (P1, P4, P6, and P8) and enriched using CD73-based MACS to identify the best developmental stage for integration following subretinal transplantation. Subsequently, CD73⁺ cells were transplanted into adult wild-type (C57BL/6J) mouse retinas and the integration efficiency was quantified 2 weeks postinjection (Fig. 1A, 1B). Cone-like cells integrated into the ONL of host retinas generating morphologically mature photoreceptors with properly located cell bodies in the ONL, apically located inner segments, and synaptic terminals in the OPL (Fig. 1B). Integration efficiency occurred in an age-dependent manner, with a peak when integrated donor cells were isolated at P4 and reduced integration levels at P1, P6, and P8 (P1: 257 ± 51 [*n* = 6]; P4: 893 ± 314 [*n* = 7]; P6: 665 ± 245 [*n* = 8]; P8: 197 ± 28 [*n* = 7]) (mean ± SEM) (Fig. 1C). Although not significantly different, donor cells were isolated at P4 for all further experiments to reduce variability. Furthermore, integrated donor cells expressed the cone-specific markers s-opsin, cone-arrestin, PNA, the pan-photoreceptor marker recoverin (Supporting Information Fig. S4A–S4H), and the presynaptic markers bassoon and synaptophysin (Supporting Information Fig. S4I, S4J). All future studies were performed using CD73-based MAC-sorted P4 *tg(Nrl*^{-/-}; aGFP) cells.

Cone-Like Photoreceptors Integrate into a Cone Degeneration Model and in a Rodless Mouse Retina

To evaluate whether cone-like photoreceptors have the capability to integrate also into retinas characterized by cone photoreceptor degeneration, an achromatopsia mouse model, the cone photoreceptor function loss 1 (*Cpfl1*) mutant, was used. *Cpfl1* mice result from a spontaneous occurring point mutation in the phosphodiesterase 6C gene (*PDE6C*), impairing cone function from 3 weeks onwards [23] (Supporting Information Fig. S2). Four weeks after transplantation, cone-like photoreceptors had properly integrated into the ONL of adult *Cpfl1* hosts, forming nuclei with multiple heterochromatin foci, inner- and outer-segments, and synaptic terminals (Figs. 2A, 3), in similar numbers to the integration into wild-type hosts (*Cpfl1* mutant: 1,359 ± 207 [*n* = 11]; wild-type: 804 ± 137 [*n* = 8] [mean ± SEM]) (Fig. 1D). The majority of transplanted cone-like photoreceptors expressed the cone-specific markers s-opsin, cone arrestin, PNA, besides the pan-photoreceptor marker recoverin (Fig. 2B–2I), and generated synaptic terminals that displayed synaptophysin and bassoon positivity (Fig. 2J, 2J(a), 2K). Additionally, the synaptic terminals of transplanted cone-like photoreceptors were located in close proximity to the dendrites of secretagogin-positive cone bipolar and calbindin-positive horizontal cells (Supporting Information Fig. S5). Ultrastructural evaluation of integrated donor cells by correlative light and electron-microscopy revealed a mature photoreceptor morphology (Fig. 3). Donor-

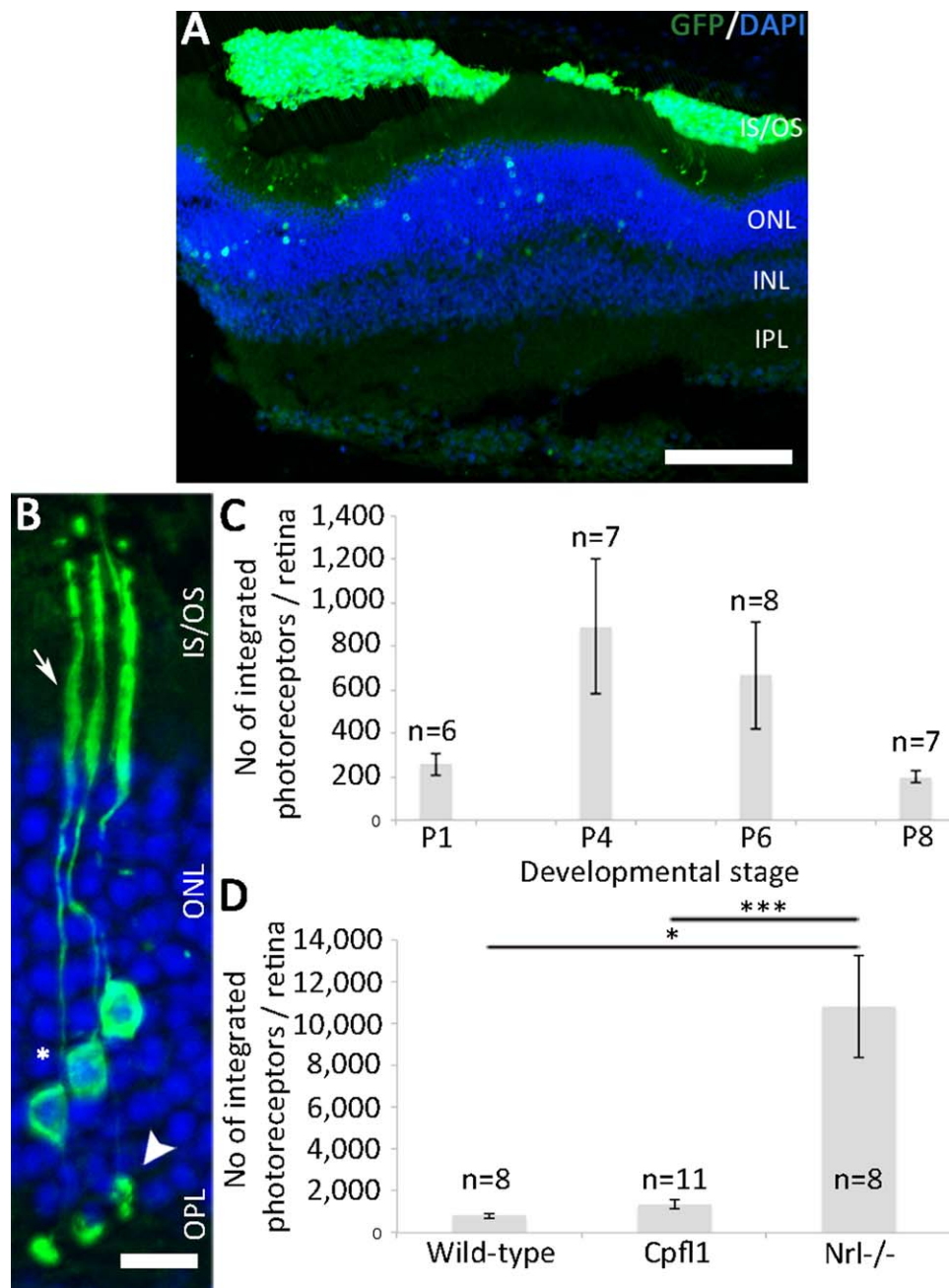


Figure 1. Transplantation of cone-like photoreceptors into different host retinas. **(A):** Overview of the retinal area containing transplanted donor cells. The remaining areas of the retina lack transplanted cone-like photoreceptors. Scale bar (A) 100 μ m. **(B):** Morphological characterization of integrated cone-like photoreceptors 2 weeks following transplantation into the adult retina of wild-type mice. Integrated cone-like cells acquired the morphology of mature photoreceptors with their cell bodies (star) located in the ONL, apical inner segments (arrow), and synaptic terminals within the OPL (arrowhead). Scale bar (B) 10 μ m. **(C):** Cone-like cells integrated in an age-dependent fashion with a peak of integration when isolated at postnatal day 4 (P4). **(D):** The integration rate of cone-like photoreceptors was quantified and compared 4 weeks following transplantation into wild-type, Cpf1 mutant, and Nrl^{-/-} hosts. While in wild-type and Cpf1 mutant mice retinas showed similar integration rates of cone-like photoreceptors, a significant \sim 13-fold increase of integrated donor cells was observed in Nrl^{-/-} hosts (n = number of eyes; *, p value < .05 or Cpf1 retinas ***, p value < .001, Student's t test, paired, two-tailed). Abbreviations: DAPI, 4',6-diamidino-2-phenylindole; GFP, green fluorescent protein; INL, inner nuclear layer; IS/OS, inner segment/outer segment; ONL, outer nuclear layer; OPL, outer plexiform layer.

derived inner segments contained mitochondria and multivesicular bodies (Fig. 3E–3G) and outer segments were filled with regular, well-aligned disc membrane staples (Fig. 3H, 3I).

Cone-like photoreceptors correctly integrated into the rod-dominated Cpf1 environment, which does not relate to a

pure cone photoreceptor environment such as the human macula. Thus, transplantations into cone-only Nrl^{-/-} mice were performed and the integration efficiency of cone-like photoreceptors was assessed after 4 weeks. Interestingly, a significant increase in the number of integrated donor cells

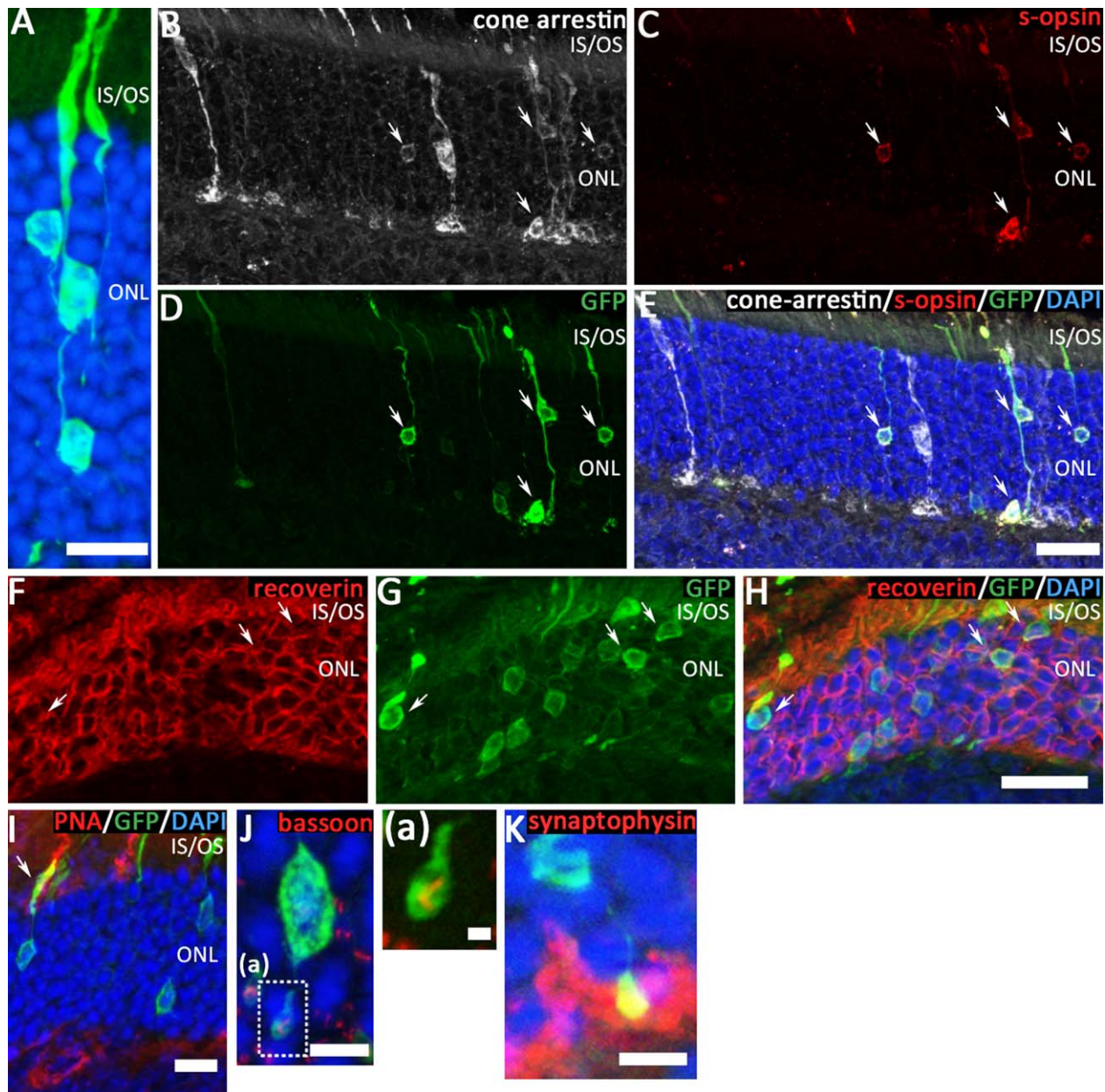


Figure 2. Integrated cone-like cells express cone-specific markers. Following transplantation into the *Cpfl1* mutant mouse retina, cone-like photoreceptors integrated into the ONL (A–K, arrows; E is a merged image of B, C, D and DAPI [blue]) and expressed cone-specific markers including cone arrestin (B, E), blue opsin (C, E), PNA (I), and the pan-photoreceptor marker recoverin (F–H) (H is a merge image of F, G and DAPI (blue)). Synaptic terminals of integrated cone-like photoreceptors expressed synaptic markers such as the ribbon marker bassoon (J, J(a)), displaying the characteristic horseshoe shape (J(a)), and synaptophysin (K). Scale bar in (A) 10 μ m; (E) (for B–E), (H) (for F–H) 20 μ m; (I) 10 μ m; (J), (K) 5 μ m; (a) 1 μ m. Abbreviations: DAPI, 4',6-diamidino-2-phenylindole; GFP, green fluorescent protein; IS/OS, inner segment/outer segment; ONL, outer nuclear layer; PNA, peanut agglutinin.

(10,829 \pm 2,446 [$n = 7$] [mean \pm SEM]) was observed when compared with wild-type (*, p value $< .05$) or *Cpfl1* (***, p value $< .001$) hosts (Fig. 1D). Integrated cone-like photoreceptors showed cone morphological features (Supporting Information Fig. S6) and expressed cone-specific markers (Supporting Information Fig. S7). Moreover, we observed that donor cells integrated in a patchy manner showed by the integrated donor cells in column-like organization (Supporting Information Fig. S6B). Interestingly, nonintegrated donor cells remaining in the subretinal space had a highly polarized mor-

phology, projecting processes toward the outer limiting membrane (OLM) (Supporting Information Fig. S6C, S6C(a)).

CD68⁺ve Cells Do Not Limit Cone-Like Photoreceptor Integration into *Cpfl1* Mice

In spite of cone-like cells' ability to integrate into different hosts, in both wild-type and *Cpfl1* mice, the integration rates were low ($< 1\%$). In fact, the presence of monocytes and macrophages (CD68⁺ve cells) was frequently observed in the subretinal space of transplanted retinas (Fig. 4A–4C) [34],

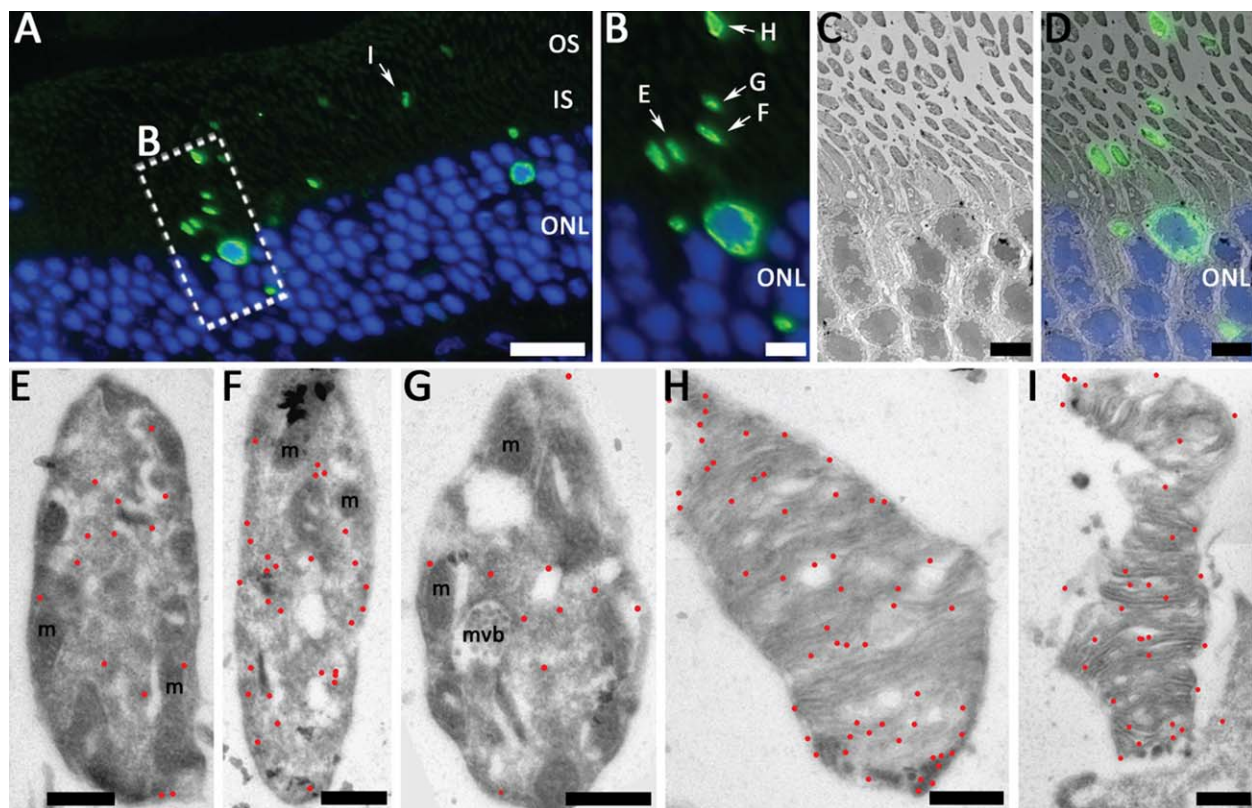


Figure 3. Ultrastructure of transplanted cone-like photoreceptors. Cone-like photoreceptors isolated from P4 $tg(Nrl^{-/-};aGFP)$ retinas were transplanted into adult $Cpfl1$ hosts and analyzed after 4 weeks by correlative light and electron microscopy. Donor cells were identified on ultrathin cryo-sections by immunohistochemistry using anti-green fluorescent protein (GFP) antibodies followed by labeling with fluorochrome-conjugated secondary antibodies (green in A, B, and D) for visualization by fluorescence microscopy and gold-conjugated Protein A (red dots in E–I) for visualization by electron-microscopy. Donor photoreceptors displayed cell bodies and cellular compartments, reminiscent of inner- and outer-segments, within and apically to the host ONL (green in A, B, D; C is the corresponding EM picture of B and D; B is the dashed box area in A). Ultra-structural analysis revealed the generation of mitochondria-containing inner- (E–G) and discs-filled outer- (H, I) segments. Letters in A and B indicate the cellular structures that are displayed in E–I by electron-microscopy. Scale bar in (A) 20 μm ; (B–D) 5 μm ; (E–I) 0.5 μm . Abbreviations: IS, inner segment; m, mitochondria; mvb, multivesicular body; ONL, outer nuclear layer; OS, outer segment.

indicative for an immune response that might influence donor cell integration. Using the same animal cohort of transplanted $Cpfl1$ mice, $CD68^{+ve}$ cells were quantified and correlated to the total number of integrated cone-like photoreceptors. No correlation between the number of $CD68^{+ve}$ cells and integrated cone-like photoreceptors was observed, suggesting that the presence of monocytes and macrophages did not interfere with the integration of cone-like photoreceptors (Fig. 4D).

The Number of Donor Photoreceptors Within the Host Retina Decreases Over Time

Long-term survival of donor cone-like photoreceptors was evaluated in wild-type and $Cpfl1$ hosts. Experimental animals were transplanted with CD73-based MACS $tg(Nrl^{-/-};aGFP)$ P4 cells and the number of integrated cone-like cells was quantified 1, 3, and 6 months following injection. Integration efficiency and survival dynamics of donor cells were similar in both, wild-type and $Cpfl1$, hosts (Fig. 4E). The total number of integrated cone-like photoreceptors significantly decreased over time from 1 month ($Cpfl1$: $1,359 \pm 207$ [$n = 11$]; wild-type: 804 ± 137 [$n = 8$]), to 3 months ($Cpfl1$: 561 ± 138 [$n = 9$]; wild-type: 424 ± 129 [$n = 7$]) and 6 months ($Cpfl1$: 336 ± 94 [$n = 9$]; wild-type: 277 ± 30 [$n = 7$] [mean \pm SEM])

in both mouse lines. Taken together, although cone-like photoreceptors can survive for prolonged time periods (at least 6 months) after transplantation in the host tissue their numbers significantly decrease over time.

Transplanted Cone-Like Photoreceptors Functionally Integrate into the $Cpfl1$ Retinal Circuitry

To evaluate the functional integration of cone-like photoreceptors 4 weeks after transplantation into $Cpfl1$ mutants, the light-mediated spiking activity of individual RGCs was recorded by microelectrode arrays. Therefore, light flashes of different intensities were presented to explanted wild-type (C75BL/6J) retinas (as an experimental reference of a healthy retina; Fig. 5A) and to $Cpfl1$ retinas in different experimental conditions: nontransplanted, sham-injected (MACS buffer), and transplanted with rod- or cone-like photoreceptors (Fig. 5; Supporting Information Fig. S8). Light-mediated responses were determined by stimulating the retina with three increasing light intensities (10, 66, and 280 mW/m^2) to separate rod (scotopic) and cone (photopic) function. Both, wild-type (Fig. 5A) and untreated $Cpfl1$ (Fig. 5; Supporting Information Fig. S8A) retinas, showed robust responses to low and medium light stimuli with 10 and 66 mW/m^2 , respectively. All classes of RGCs (ON, ON-OFF, and OFF) were detected in all measurements. In contrast, at high light

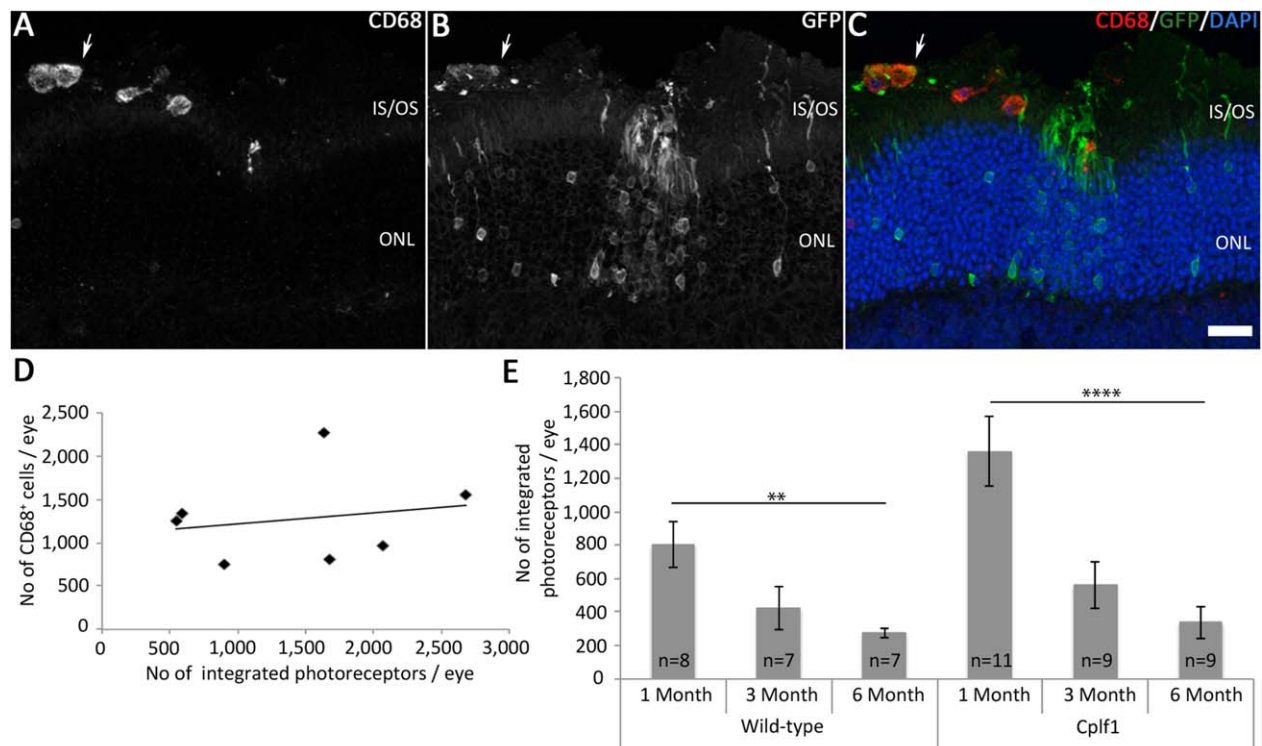


Figure 4. Host response to integrated transplanted cone-like cells and their long-term survival. Immunohistochemical labeling of CD68⁺ cells (A, C, arrows; C is a merged image of A and B plus DAPI [blue]) in transplanted Cpf1 retinas revealed the presence of monocytes/macrophages in the subretinal space in close proximity to integrated donor cells (A–C, arrow). Some CD68-positive monocytes/macrophages contained internalized GFP particles (B, C). Correlation analysis between the number of integrated cone-like photoreceptors and the number of CD68⁺ cells in the host retinas revealed that CD68⁺ cells did not interfere with the integration rate of donor cells ($n = 7$) (D). Integrated cone-like photoreceptors survived for up to 6 months following transplantation in wild-type and Cpf1 mutant hosts (E), but their number significantly decreased over time with similar dynamics in both analyzed mouse lines (****, $p < .0005$; **, $p < .01$; one-way ANOVA) (E). Scale bar in C (for A–C) 20 μm . Abbreviations: DAPI, 4',6-diamidino-2-phenylindole; GFP, green fluorescent protein; IS, inner segment; ONL, outer nuclear layer; OS, outer segment.

intensities (photopic, 280 mW/m^2) only wild-type (Fig. 5A) but not untreated Cpf1 (Fig. 5; Supporting Information Fig. S8A) retinas responded to the light stimuli, demonstrating impaired cone photoreceptor function. Similarly, following sham-injection (Fig. 5B, 5D) or transplantation with P4 rod photoreceptor precursors (Supporting Information Figs. S8B, S9), Cpf1 retinas showed robust RGC responses to low and medium light intensities but no response to stimuli with high light intensities. Specifically, all recorded RGCs in the referred conditions responded at each of the 15 stimulus repetitions at low light intensity but none at high light intensity (Fig. 5; Supporting Information Fig. S8). In contrast, light-induced spikes from RGCs in Cpf1 retinas transplanted with cone-like photoreceptors were detected at all the three tested light intensities (Fig. 5C). In fact, out of 54 recorded RGCs 20 (37%) responded to high (photopic) light levels and all major cell classes (ON, ON-OFF, and OFF RGCs) were identified in Cpf1 retinas containing transplanted cone-like photoreceptors (Fig. 5C, 5D). No statistical comparison was performed for the electrophysiological recordings as in control photopic conditions the number of responsive cells was zero.

DISCUSSION

The development of therapeutic interventions to restore daylight vision is of prime importance given the high incidence of

retinal diseases characterized by cone photoreceptor loss, such as late stage RP, cone-rod dystrophies, and AMD. In fact, AMD is the leading cause of blindness in industrialized countries. The evaluation of cell replacement therapies for such conditions is impeded due the lack of sufficient numbers of cone photoreceptors for detailed preclinical transplantation studies. Therefore, cone-only retinas of $\text{Nr1}^{-/-}$ mice were used as a comprehensive source of donor cells to establish a proof-of-concept for functional rescue of daylight responses following cell transplantation into a cone photoreceptor degeneration mouse model.

The generated cone-like photoreceptor reporter line, $\text{tg}(\text{Nr1}^{-/-}; \text{aGFP})$, displayed all the hallmarks of the $\text{Nr1}^{-/-}$ phenotype at the histological and physiological level demonstrated by the expression of cone-specific markers within virtually all photoreceptors and the lack of rod-mediated light responses with preserved cone photoreceptor function. Additionally, CD73 was identified as a cell surface antigen expressed in cone-like photoreceptors as described in previously published microarray analysis [26], allowing MACS-based enrichment as previously established for rod transplantation [7, 13]. CD73-based MAC-sorting resulted in cell fractions containing ~80% cone-like photoreceptors, representing a lower purification rate than for CD73-based MAC-sorted rods (~90% [13]) and might result from reduced expression levels of CD73 in cone-like photoreceptors [26], which is supported by the

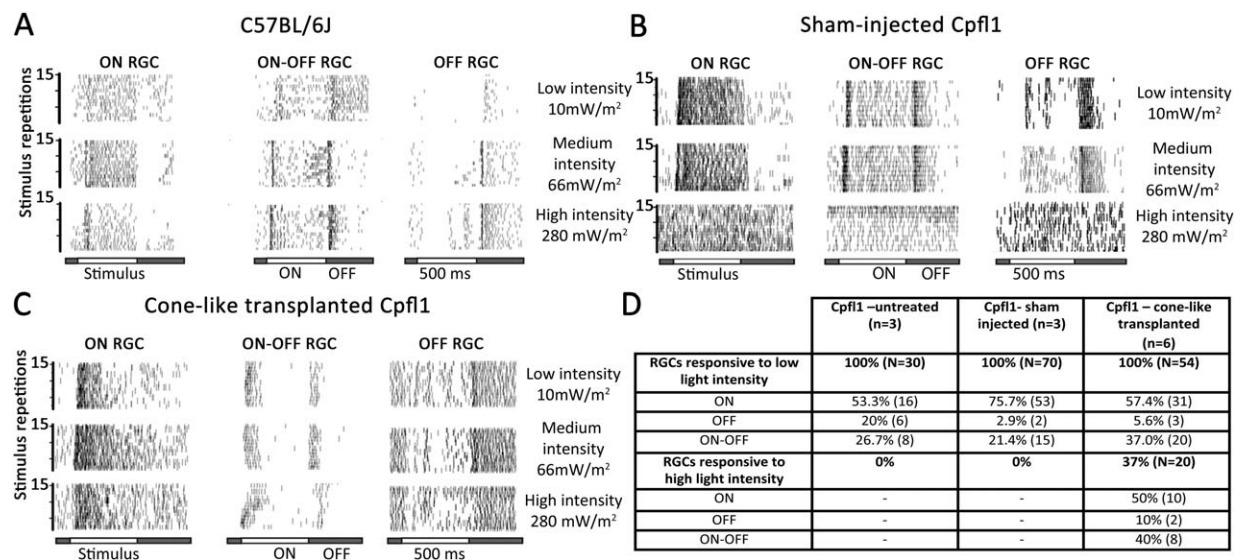


Figure 5. Functional integration of cone-like photoreceptors into Cpf11 retinas. Representative microelectrode array (MEA) recordings performed on RGCs of wild-type (C57BL/6J) (A) and Cpf11 retinas 4 weeks following sham injection (B) or transplantation of cone-like photoreceptors (C) are shown. Each tick represents the occurrence of one action potential (spike). RGC spiking was recorded on MEAs during stimulation with repetitive light flashes of 500 milliseconds duration. The flickering (1 Hz) stimulus was presented 15 times at each of three different light intensities. At low and medium light intensities, robust responses characteristic for ON, ON-OFF, and OFF RGCs were detected in wild-type (A), sham-injected (B), and cone-like photoreceptor transplanted (C) Cpf11 retinas. During the presentation of high light intensity (photopic) flashes, an increase in spontaneous activity but no specific stimulus-driven responses, as seen in wild-type retinas (A), were detectable in sham-injected (B, D). In contrast, Cpf11 retinas, containing transplanted cone-like photoreceptors (C), showed characteristic stimulus-driven responses in ON, ON-OFF, and OFF RGCs under high light intensity conditions. (D): Summary of the recorded RGC subtypes for each light intensity in Cpf11-untreated (Supporting Information Fig. S8), sham-injected Cpf11, and cone-like transplanted Cpf11 retinas. At high light intensity RGC responses were recorded in cone-like transplanted Cpf11 retinas only. n = number of retinas; N = number of cells. Abbreviation: RGC, retinal ganglion cell.

suggested low CD73 expression in neonatal primary cone photoreceptor precursors [33].

Following transplantation, a fraction of donor cone-like photoreceptors properly integrated into the ONL of hosts, presenting the morphology of mature photoreceptors including inner- and outer segments, nuclei with several heterochromatin foci, and synaptic terminals beside the expression of pan-photoreceptor (recoverin) and cone-specific markers (cone arrestin, PNA, and s-opsin). Integrated cone-like photoreceptors expressed the presynaptic markers bassoon and synaptophysin and their synaptic terminals were located in close proximity to the dendrites of cone bipolar and horizontal cells, presumptive evidence for functional synaptic terminals. Cone-like photoreceptors displayed a similar integration mode as primary rod- [6, 7, 9–13, 17, 18] or cone photoreceptors [19]. The mature photoreceptor morphology of cone-like cells was observed following transplantation into all transplanted mouse lines. Interestingly, the size of synaptic terminals of integrated cone-like photoreceptors was often similar to rod spherules and only sometimes resembled large cone pedicles (Figs. 1B, 2A). This observation might be explained by the s-cone phenotype of $Nrl^{-/-}$ photoreceptors as cone photoreceptors solely expressing s-opsin also display a smaller cone pedicle size in comparison to the other cone photoreceptor subtypes [35].

Mis-localization of s-opsin throughout the cell body was observed in integrated cone-like photoreceptors, however, without affecting their function as demonstrated by RGC recordings. Furthermore, although the majority of integrated donor photoreceptors expressed cone-specific markers, some integrated cone-like photoreceptors showed no/low expres-

sion of PNA or cone arrestin, which might be indicative for incomplete maturation of donor cells, as they were isolated during development at P4. Alternatively, some donor photoreceptors might have started to degenerate, a condition characterized by mis-expression/-localization of opsins as seen in several inherited or induced retinal disease models. Indeed, a decrease of integrated donor cells was observed in our long-term studies. However, virtually all donor photoreceptors that had integrated into the ONL of wild-type or Cpf11 recipients displayed a mature photoreceptor morphology including proper inner- and outer segments. In contrast, within $Nrl^{-/-}$ retinas endogenous photoreceptors showed a slightly disrupted morphology with the presence of shorter inner- and outer segments (OSs) containing atypical disks [22, 36]. These observations suggest that the formation of proper photoreceptor morphology is not intrinsically impaired in cone-like photoreceptors but instead is highly influenced by environmental factors.

Interestingly, nonintegrated cone-like photoreceptors remaining in the subretinal space of $Nrl^{-/-}$ hosts displayed a highly polarized morphology, a feature not observed in wild-type or Cpf11 hosts. The $Nrl^{-/-}$ retinal architecture may contribute to this phenotype as photoreceptor OS-retinal pigment epithelium (RPE) contacts are significantly reduced in $Nrl^{-/-}$ mice when compared with wild-type mice [36], in which endogenous photoreceptors display OSs tightly packed, cylindrically arranged, and with proper contacts to the RPE [21, 22, 36]. Following cell transplantation, this retinal architecture might promote a solid reattachment between photoreceptor OSs and RPE microvilli, resulting in clusters of nonintegrated and nonpolarized cells lying in the subretinal space. Thus, in

the $Nrl^{-/-}$ hosts reduced OS-RPE contacts [36] may contribute to a weaker retinal reattachment with reduced physical constraints allowing donor cells to achieve a polarized morphology with oriented projections toward the OLM.

The integration rates into the ONL of both, wild-type and Cpf1 mutant mice, were low (<1%) representing a major hurdle for cell replacement approaches. Such low integration rates were also observed following transplantation of rod photoreceptors [9, 10]. However, several factors have been identified that influence integration success including the outer limiting membrane, extracellular matrix, or reactive gliosis and modulation of these components positively affected the integration rate of donor rods to up to 10% [6, 11, 12, 18]. Furthermore, an immune response following photoreceptor transplantation might also represent a limiting factor for donor cell integration. However, no direct correlation between the low number of integrated cone-like photoreceptors and the high number of CD68⁺ve macrophages and monocytes present in the subretinal space 1 month after transplantation was observed. This data are in accordance with previous results using rod photoreceptors, demonstrating that macrophage and monocyte invasion are a consequence of the transplantation process and not a limiting factor for integration. Nonetheless, long-term survival of donor photoreceptors might be restricted due to rejection mechanisms of the host [34]. In fact, we observed a decrease of the total number of integrated cone-like photoreceptors from 1 to 3 and 6 months both in wild-type and Cpf1 mutant mice. This decline might not be fully attributed to the host response, since $Nrl^{-/-}$ mice also show a transient photoreceptor degeneration [37]. Additionally, mis-localization of opsins to the photoreceptor cell body might trigger apoptosis of transplanted donor cells, as a recent study showed that accumulation of rhodopsin in the cell body of rods triggers photoreceptor death [38]. Thus, the exact cause for the decrease of integrated cone-like photoreceptors over time remains to be clarified.

Transplanted donor cells displayed similar integration efficiencies in wild-type and Cpf1 hosts but a ~13-fold higher integration rate in the ONL of $Nrl^{-/-}$ mice. $Nrl^{-/-}$ retinas have a disrupted outer limiting membrane [39] and display transient photoreceptor degeneration [37], conditions that were previously shown to facilitate integration of rod photoreceptors [11, 18], confirming that the host environment is crucial for the integration rate of subretinally transplanted photoreceptors. Additionally, the cell bodies forming the ONL are less tightly packed in $Nrl^{-/-}$ mice [22] than in wild-type or Cpf1 retinas and might represent a more permissive environment for donor photoreceptor integration.

Correct integration of donor photoreceptors into the host neural circuitry and restoration of visual function represents the ultimate goal of cell replacement approaches in the retina. Indeed, recent studies demonstrated some improvements in visual function following transplantation of rod photoreceptors into mouse models of RP, based on visual-stimulated reflexive or behavioral tests [6, 7, 18]. However, the low number of integrated donor photoreceptors within the host tissue is still a major barrier for the evaluation of significant visual improvements by standard ophthalmology functional tests like ERG [6] and indeed we could not detect changes in ERG amplitudes in Cpf1 mice transplanted with cone-like photore-

ceptors (data not shown). Therefore, microelectrode arrays were used in this study to record multiple individual RGC responses upon light stimulation, allowing to investigate functional consequences also by small numbers of integrated photoreceptors. Indeed, in the cone-depleted retinas of Cpf1 mice responses to photopic stimuli were undetectable. However, following transplantation of cone-like photoreceptors robust responses were measured in Cpf1 retinas following presentation of photopic light stimuli, providing the first evidence for functional integration and connection of daylight-sensing photoreceptors into the retinal circuitry of a cone degeneration mouse model. A neuroprotective effect of donor cells on remaining endogenous cones, as a theoretical alternative explanation for the observed photopic light responses, seems unlikely, given the age of experimental Cpf1 mice at the time of transplantation, that was considerably after the detection of any cone functionality [23]. Additionally, transplantation of rod photoreceptors did not lead to functional improvements. Actually, protective effectors for the reactivation of cones impaired by mutations in a key factor of the light transduction cascade, that is, PDE, have not been described so far [40].

Analyzing functional integration of transplanted photoreceptors by microelectrode arrays further allows the evaluation of their contribution to ON and OFF pathways. Indeed, similar numbers of ON and OFF RGCs with reduced numbers of ON-OFF RGCs were detected following transplantation, representing a pattern similar to the wild-type retina [35, 41]. These results emphasize the importance for detailed analysis of generated connections by donor photoreceptors to endogenous neurons, once correct retinal circuits are essential for the proper processing and transmission of visual stimuli within the retina and to the brain. Further in depth investigations at the cellular level will help to determine the exact cell-type to which transplanted photoreceptors are synaptically connected and whether cell-cell communication is established to neighboring photoreceptors. Such approaches would provide insights into the correct re-establishment of the degenerated retinal circuitry, fulfilling the ultimate objective of photoreceptor replacement therapies.

CONCLUSIONS

Replacement of photoreceptors by transplantation represents a promising strategy for the treatment of incurable retinal diseases. Here, we provide the proof-of-concept for restoration of daylight vision following transplantation of cone-like photoreceptors into a mouse model of cone degeneration. As primary and genetically engineered photoreceptors isolated from the developmental retina do not represent a reliable donor cell source in a clinical setting, the establishment of an in vitro expandable cell source for providing transplantable cone photoreceptors will be mandatory. In fact, the successful in vitro generation of photoreceptors from mouse and human induced pluripotent- and embryonic stem cells [8, 16, 42–50] represents a major step toward the availability of sufficient donor material for transplantation studies. However, the development of techniques for the efficient differentiation of stem cells along the cone lineage and identification of cone-specific cell surface markers for their enrichment will be vital

for bringing photoreceptor replacement strategies closer toward clinical application with the aim to treat cone retinopathies.

ACKNOWLEDGMENTS

This work was supported by the Deutsche Forschungsgemeinschaft (DFG) FZT 111 (Center for Regenerative Therapies Dresden, Cluster of Excellence), DFG Grant AD375/3-1, DFG Sonderforschungsbereich 655 "From cells into tissue" (Grant 041_296318), the Fundação para a Ciência e a Tecnologia (FCT: SFRH/BD/60787/2009), and the ProRetina Stiftung. We thank Anand Swaroop and Sandra Cottet for providing Nr^{-/-} mice, Bernd Wissinger for providing Cpf1 mice, Wolfgang Baehr for cone arrestin antibody, Jochen Haas and Susanne Kretschmar for technical support, and Sindy Böhme, Emily Lessmann, and Katrin Baumgart for animal husbandry.

AUTHOR CONTRIBUTIONS

T.S.-F.: conception and design, collection and assembly of data, data analysis and interpretation, and manuscript writing; K.P.: collection and assembly of data; H.S.: collection and assembly of data and data analysis and interpretation; T.K.: collection and assembly of data, data analysis and interpretation, and manuscript writing; G.Z.: conception and design, data analysis and interpretation, and manuscript writing; M.A.: conception and design, data analysis and interpretation, financial support, manuscript writing, and final approval of manuscript.

DISCLOSURE OF POTENTIAL CONFLICTS OF INTEREST

The authors indicate no potential conflicts of interest.

REFERENCES

- Berger W, Kloeckener-Gruissem B, Neidhardt J. The molecular basis of human retinal and vitreoretinal diseases. *Prog Retin Eye Res* 2010;29:335–375.
- Swaroop A, Chew EY, Rickman CB et al. Unraveling a multifactorial late-onset disease: From genetic susceptibility to disease mechanisms for age-related macular degeneration. *Annu Rev Genomics Hum Genet* 2009;10:19–43.
- Ramsden CM, Powner MB, Carr A-JF et al. Stem cells in retinal regeneration: Past, present and future. *Development* 2013;140:2576–2585.
- Petrs-Silva H, Linden R. Advances in gene therapy technologies to treat retinitis pigmentosa. *Clin Ophthalmol* 2014;8:127–136.
- Cideciyan AV, Aleman TS, Boye SL et al. Human gene therapy for RPE65 isomerase deficiency activates the retinoid cycle of vision but with slow rod kinetics. *Proc Natl Acad Sci USA* 2008;105:15112–15117.
- Pearson RA, Barber AC, Rizzi M et al. Restoration of vision after transplantation of photoreceptors. *Nature* 2012;485:99–103.
- Singh MS, Charbel Issa P, Butler R et al. Reversal of end-stage retinal degeneration and restoration of visual function by photoreceptor transplantation. *Proc Natl Acad Sci USA* 2013;110:1101–1106.
- Homma K, Okamoto S, Mandai M et al. Developing rods transplanted into the degenerating retina of crx-knockout mice exhibit neural activity similar to native photoreceptors. *STEM CELLS* 2013;31:1149–1159.
- Bartsch U, Oriyakhel W, Kenna PF et al. Retinal cells integrate into the outer nuclear layer and differentiate into mature photoreceptors after subretinal transplantation into adult mice. *Exp Eye Res* 2008;86:691–700.
- MacLaren RE, Pearson RA, MacNeil A et al. Retinal repair by transplantation of photoreceptor precursors. *Nature* 2006;444:203–207.
- West EL, Pearson RA, Tschernutter M et al. Pharmacological disruption of the outer limiting membrane leads to increased retinal integration of transplanted photoreceptor precursors. *Exp Eye Res* 2008;86:601–611.
- Pearson RA, Barber AC, West EL et al. Targeted disruption of outer limiting membrane junctional proteins (Crb1 and ZO-1) increases integration of transplanted photoreceptor precursors into the adult wild-type and degenerating retina. *Cell Transplant* 2010;19:487–503.
- Eberle D, Schubert S, Postel K et al. Increased integration of transplanted CD73-positive photoreceptor precursors into adult mouse retina. *Invest Ophthalmol Vis Sci* 2011;52:6462–6471.
- Eberle D, Kurth T, Santos-Ferreira T et al. Outer segment formation of transplanted photoreceptor precursor cells. *PLoS One* 2012;7:e46305.
- West EL, Pearson RA, Duran Y et al. Manipulation of the recipient retinal environment by ectopic expression of neurotrophic growth factors can improve transplanted photoreceptor integration and survival. *Cell Transplant* 2012;21:871–887.
- Gonzalez-Cordero A, West EL, Pearson RA et al. Photoreceptor precursors derived from three-dimensional embryonic stem cell cultures integrate and mature within adult degenerate retina. *Nat Biotechnol* 2013;31:741–747.
- Lakowski J, Han Y-T, Pearson RA et al. Effective transplantation of photoreceptor precursor cells selected via cell surface antigen expression. *STEM CELLS* 2011;29:1391–1404.
- Barber AC, Hippert C, Duran Y et al. Repair of the degenerate retina by photoreceptor transplantation. *Proc Natl Acad Sci USA* 2013;110:354–359.
- Lakowski J, Baron M, Bainbridge J et al. Cone and rod photoreceptor transplantation in models of the childhood retinopathy Leber congenital amaurosis using flow-sorted Crx-positive donor cells. *Hum Mol Genet* 2010;19:4545–4559.
- Jeon CJ, Strettoi E, Masland RH. The major cell populations of the mouse retina. *J Neurosci* 1998;18:8936–8946.
- Mears AJ, Kondo M, Swain PK et al. Nrl is required for rod photoreceptor development. *Nat Genet* 2001;29:447–452.
- Daniele LL, Lillo C, Lyubarsky AL et al. Cone-like morphological, molecular, and electrophysiological features of the photoreceptors of the Nrl knockout mouse. *Invest Ophthalmol Vis Sci* 2005;46:2156–2167.
- Chang B, Hawes NL, Hurd RE et al. Retinal degeneration mutants in the mouse. *Vision Res* 2002;42:517–525.
- Okabe M, Ikawa M, Kominami K et al. "Green mice" as a source of ubiquitous green cells. *FEBS Lett* 1997;407:313–319.
- Eberle D, Santos-Ferreira T, Grahl S et al. Subretinal transplantation of MACS purified photoreceptor precursor cells into the adult mouse retina. *J Vis Exp* 2014;(84):e50932.
- Akimoto M, Cheng H, Zhu D et al. Targeting of GFP to newborn rods by Nrl promoter and temporal expression profiling of flow-sorted photoreceptors. *Proc Natl Acad Sci USA* 2006;103:3890–3895.
- Tokuyasu KT. Immunocytochemistry on ultrathin frozen sections. *Histochem J* 1980;12:381–403.
- Slot JW, Geuze HJ. Cryosectioning and immunolabeling. *Nat Protoc* 2007;2:2480–2491.
- Fabig G, Kretschmar S, Weiche S et al. Labeling of ultrathin resin sections for correlative light and electron microscopy. *Methods Cell Biol* 2012;111:75–93.
- Vicidomini G, Gagliani MC, Canfora M et al. High data output and automated 3D correlative light-electron microscopy method. *Traffic* 2008;9:1828–1838.
- Stutzki H, Leibig C, Andreadaki A et al. Inflammatory stimulation preserves physiological properties of retinal ganglion cells after optic nerve injury. *Front Cell Neurosci* 2014;8:38.
- Harris KD, Henze DA, Csicsvari J et al. Accuracy of tetraode spike separation as determined by simultaneous intracellular and extracellular measurements. *J Neurophysiol* 2000;84:401–414.
- Koso H, Minami C, Tabata Y et al. CD73, a novel cell surface antigen that characterizes retinal photoreceptor precursor cells. *Invest Ophthalmol Vis Sci* 2009;50:5411–5418.
- West EL, Pearson RA, Barker SE et al. Long-term survival of photoreceptors transplanted into the adult murine neural retina requires immune modulation. *STEM CELLS* 2010;28:1997–2007.

- 35** Breuninger T, Puller C, Haverkamp S et al. Chromatic bipolar cell pathways in the mouse retina. *J Neurosci* 2011;31:6504–6517.
- 36** Mustafi D, Kevany BM, Genoud C et al. Defective photoreceptor phagocytosis in a mouse model of enhanced S-cone syndrome causes progressive retinal degeneration. *FASEB J* 2011;25:3157–3176.
- 37** Roger JE, Ranganath K, Zhao L et al. Preservation of cone photoreceptors after a rapid yet transient degeneration and remodeling in cone-only *Nrl*^{-/-} mouse retina. *J Neurosci* 2012;32:528–541.
- 38** Chinchore Y, Mitra A, Dolph PJ. Accumulation of rhodopsin in late endosomes triggers photoreceptor cell degeneration. *PLoS Genet* 2009;5:e1000377.
- 39** Stuck MW, Conley SM, Naash MI. Defects in the outer limiting membrane are associated with rosette development in the *Nrl*^{-/-} retina. *PLoS One* 2012;7:e32484.
- 40** Trifunović D, Sahaboglu A, Kaur J et al. Neuroprotective strategies for the treatment of inherited photoreceptor degeneration. *Curr Mol Med* 2012;12:598–612.
- 41** Haverkamp S, Wässle H, Duebel J et al. The primordial, blue-cone color system of the mouse retina. *J Neurosci* 2005;25:5438–5445.
- 42** Lamba DA, Gust J, Reh TA. Transplantation of human embryonic stem cell-derived photoreceptors restores some visual function in *Crx*-deficient mice. *Cell Stem Cell* 2009;4:73–79.
- 43** Lamba DA, McUsic A, Hirata RK et al. Generation, purification and transplantation of photoreceptors derived from human induced pluripotent stem cells. *PLoS One* 2010;5:e8763.
- 44** Eiraku M, Takata N, Ishibashi H et al. Self-organizing optic-cup morphogenesis in three-dimensional culture. *Nature* 2011;472:51–56.
- 45** Eiraku M, Sasai Y. Mouse embryonic stem cell culture for generation of three-dimensional retinal and cortical tissues. *Nat Protoc* 2012;7:69–79.
- 46** Nakano T, Ando S, Takata N et al. Self-formation of optic cups and storable stratified neural retina from human ESCs. *Cell Stem Cell* 2012;10:771–785.
- 47** West EL, Gonzalez-Cordero A, Hippert C et al. Defining the integration capacity of embryonic stem cell-derived photoreceptor precursors. *STEM CELLS* 2012;30:1424–1435.
- 48** Hirami Y, Osakada F, Takahashi K et al. Generation of retinal cells from mouse and human induced pluripotent stem cells. *Neurosci Lett* 2009;458:126–131.
- 49** Tucker BA, Park I-H, Qi SD et al. Transplantation of adult mouse iPS cell-derived photoreceptor precursors restores retinal structure and function in degenerative mice. *PLoS One* 2011;6:e18992.
- 50** Meyer JS, Howden SE, Wallace KA et al. Optic vesicle-like structures derived from human pluripotent stem cells facilitate a customized approach to retinal disease treatment. *STEM CELLS* 2011;29:1206–1218.



See www.StemCells.com for supporting information available online.